Conformational Transitions in Chiral, Gallic Acid-Functionalized Poly(dithienopyrrole): A Comparative UV−vis and CD Study

Wouter Vanormelingen, Karlien Van den Bergh, Thierry Verbiest, and Guy Koeckelberghs*

Laboratory for Molecular Electronics and Photonics, Katholieke Universiteit Leuven, Celestijnenlaan 200F, B-3001 Heverlee, Belgium

Received May 30, 2008; Revised Manuscript Received June 9, 2008

ABSTRACT: An achiral and chiral poly(dithieno[3,2-*b*:2′,3′-*d*]pyrrole) (PDTP), substituted with a gallic acid-derived moiety, was prepared by a Stille coupling, and the supramolecular behavior in solution was studied. In a good solvent (THF), the polymers are present as unordered, highly conjugated, rigid-rod-like strands. Upon addition of a nonsolvent (hexane) or in toluene, the polymer strands adopt a helical conformation in contrast to previously reported alkyl-substituted PDTPs, which aggregate by decreasing the solvent quality. The folding and unfolding process was investigated by probing the UV−vis and CD intensities at different wavelengths and temperatures. On the basis of these experiments, it could be concluded that the helical folding and unfolding is a single-step process. The PDTP could also be oxidized and rereduced, and thus, in principle, a molecular solenoid can be obtained.

Introduction

Over the past few decades, a lot of effort has been devoted to the development of synthetic helical polymers and oligomers. These systems are not only of interest as mimics of complex natural systems, but they can also be used as a (chiral) scaffold to align chromophores, sensory functions, catalytic sites, etc.[1,2a–c]

Also, conjugated polymers and oligomers can adopt a helical conformation. The formation of this helical conformation is often governed by secondary interactions, such as hydrogen bonding, solvophobic interactions, π-stacking, lone pair repulsions, and chalcogen−chalcogen interactions. Some examples of helical polymers and oligomers constitute substituted cis−transoid poly(acetylenes),[2] oligo(*m*-phenyleneethynylenes),[3] and oxazoline-functionalized poly(thiophene)s.[4] Unfortunately, most of these polymers exhibit a limited conjugation length.

On the other hand, most poly(thiophene)s and their derivatives, for instance poly(dithieno[3,2-*b*:2′,3′-*d*]pyrrole) (PDTP),[5] are highly conjugated polymers. PDTPs show high conjugation lengths ($\lambda_{max} \sim 550$ nm), they can easily be oxidized, and they remain oxidized for prolonged periods of time. Substitution with sufficient bulky alkyl groups renders them soluble.[5e,f] In good solvents, alkyl-substituted PDTPs are present as rigid-rod-like molecules, which stack upon decreasing the solvent quality or by transition to the solid state. Finally, if chiral substituents are employed, the polymer chains stack in a chiral way.[5d,f]

Chiral conjugated polymers, which can relatively easily be doped (oxidized), can be considered as the molecular counterpart of a solenoid. A first approach for the development of chiral polymer conductors consists of chirally stacked, dopable conjugated polymers.[5d,f,6] A second strategy, in which the relationship between chirality and conjugation is stricter, is the construction of chiral, helical polymers with a stable oxidized state. This has, for instance, been accomplished in poly(anilines) and PEDOT derivatives, which are chirally wrapped around a chiral template during polymerization.[7]

A particularly interesting group for (chiral) helical induction is a tri(alkyl)-substituted gallic acid moiety. The combination of space confinement, π-stacking, and van der Waals interactions favors a helical conformation, while the presence of chiral substituents, together with proper space confinement and the rigidity of the benzene moiety, results in an efficient discrimination of the two enantiomeric helices.[8] A very nice example of this approach is found in poly(ureidophthalimide)s.[9] Another asset of this group is its ability to increase the solubility of the polymers in common organic solvents.

In this article, (a)chiral gallic acid-functionalized PDTPs (Figure 1) are prepared. It is investigated whether the introduction of a gallic acid moiety can induce a helical conformation in these polymers. Moreover, the folding and unfolding process is investigated into detail by UV−vis and CD spectroscopy. Finally, the oxidation of the polymers is studied, demonstrating that these materials can indeed be considered as molecular solenoids.

Experimental Section

Reagents and Instrumentation. All reagents were purchased from Aldrich Chemical Co., Acros Organics, Merck, Fluka, and Avocado. When necessary, reagent grade solvents were dried and purified by distillation.

Gel permeation chromatography (GPC) measurements were done with a Shimadzu 10A apparatus with a tunable absorbance detector and a differential refractometer in tetrahydrofuran (THF) as eluent toward polystyrene standards. ^{1}H and ^{13}C nuclear magnetic resonance (NMR) measurements were carried out with a Bruker Avance 300 MHz. UV−vis and CD spectra were recorded with a Varian Cary 400 and a JASCO 62 DS apparatus, respectively. The DSC measurements were performed on a Perkin-Elmer DSC 7 apparatus. Optical rotation was done on a Polaar 20; the concentration (in g/100 mL) and solvent are given in parentheses. Cyclic voltammetry was performed on a Princeton Applied Research PARSTAT 2273, equipped with a standard three-electrode configuration. A SCE (3 M KCl) electrode served as a reference electrode and a Pt wire and disk as counter and working electrode. The measurements were done in acetonitrile with Bu_4NBF_4 (0.1 M) as

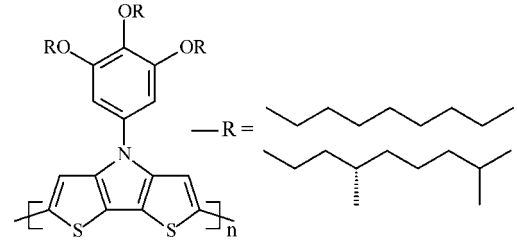

Figure 1. Structure of the polymers.

* Corresponding author. E-mail: guy.koeckelberghs@chem.kuleuven.be.

10.1021/ma8012114 CCC: $40.75
Published on Web 07/18/2008

the supporting electrolyte. Ferrocene was added before each run as an internal standard. The Fe(II/III) couple of ferrocene was observed at 0.416 V (scan rate = 50 mV/s). For the measurements, a polymer film was dropcasted on the Pt disk working electrode.

Compound **7** was prepared according to literature procedures.[10]

Synthesis of the Monomers. *Synthesis of 3,4,5-Tri(octyloxy)nitrobenzene (**2a**).* A suspension of SiO_2 (10.2 g, 170 mmol) and HNO_3 (65% in H_2O, 16.5 mL) was stirred for 10 min. Then, 1,2,3-tri(octyloxy)benzene (**1a**) (53.0 g, 115 mmol) was rapidly added. After 15 min at room temperature, the suspension was filtered. The filtrate was concentrated in vacuo and added dropwise to cold (0 °C) MeOH. The precipitate was filtered and washed two times with cold MeOH. Since the product melts near room temperature, the product was dissolved in CH_2Cl_2 and the solvent was removed by rotary evaporation, leaving a pale yellow oil. Yield: 29.8 g (51%). ^{1}H NMR ($CDCl_3$): δ = 7.47 (s, 2H), 4.03 (m, 6H), 1.70−1.91 (m, 6H), 1.48 (m, 6H), 1.29 (m, 24H), 0.88 (m, 9H).

*Synthesis of 3,4,5-Tri(octyloxy)aniline (**3a**).* $SnCl_2$ (89.0 g, 470 mmol) was added to a refluxing solution of **2a** (29.8 g, 59.0 mmol) in 500 mL of EtOH/EtOAc (1/1). After being refluxed for 2 h, the reaction mixture was allowed to cool down and poured in aqueous NaOH (1 L, 5 M). CH_2Cl_2 (300 mL) was added, and the organic layer was isolated. The remaining aqueous layer was again extracted with CH_2Cl_2 (300 mL). The combined organic layers were dried over $MgSO_4$ and, after filtration, concentrated in vacuo. Purification of the crude product by column chromatography (SiO_2, CH_2Cl_2/EtOAc (95/5)) afforded a white solid. Yield: 12.4 g (44%); mp 74−75 °C (lit. 73−74 °C).[11b] ^{1}H NMR ($CDCl_3$): δ = 5.91 (s, 2H), 3.90 (t, 4H), 3.84 (t, 2H), 3.45 (s, 2H, br), 1.64−1.83 (m, 6H), 1.45 (m, 6H), 1.28 (m, 24H), 0.88 (m, 9H).

*Synthesis of 3,4,5-Tri((S)-3,7-dimethyloctyloxy)aniline (**3b**).* The same procedure as described for **3a** was followed, starting from 3,4,5-tri((*S*)-3,7-dimethyloctyloxy)nitrobenzene (**2b**) (27.5 g, 46.5 mmol). **3b** was isolated as a yellow oil. Yield: 9.00 g (34%). ^{1}H NMR ($CDCl_3$): δ = 5.92 (s, 2H), 3.81−4.01 (m, 6H), 3.25 (s, 2H, br), 1.76−1.91 (m, 3H), 1.61−1.74 (m, 3H), 1.44−1.61 (m, 6H), 1.24−1.38 (m, 9H), 1.08−1.21 (m, 9H), 0.91 (m, 9H), 0.86 (d, J = 6.4 Hz, 18H).

*Synthesis of N-[3,4,5-Tri(octyloxy)phenyl]dithieno[3,2-b:2′,3′-d]pyrrole (**4a**).* A solution of **7** (3.00 g, 9.30 mmol), NaO*t*Bu (2.16 g, 22.5 mmol), Pd_2dba_3 (0.220 g, 0.234 mmol), and DPPF (0.519 g, 0.936 mmol) in dry toluene (15 mL) was purged with argon for 10 min. Then, **3a** (4.50 g, 9.60 mmol) was added, and the mixture was refluxed until completion of the reaction (TLC-monitoring, SiO_2, CH_2Cl_2/hexane (50/50)). Then (after 7 h) the solution was allowed to cool down, and water was added. The aqueous layer was extracted with Et_2O. The combined organic layers were dried over $MgSO_4$, and after filtration, the solvents were removed by rotary evaporation. Finally, the crude product was purified by column chromatography (SiO_2, CH_2Cl_2/hexane (50/50)) and was isolated as a colorless oil, which slowly crystallizes to a white solid. Yield: 5.10 g (86%); mp 32.9−34.7 °C. ^{1}H NMR ($CDCl_3$): δ = 7.17 (d, J = 5.5 Hz, 2H), 7.14 (d, J = 5.5 Hz, 2H), 6.75 (s, 2H), 3.99 (m, 6H), 1.88−1.73 (m, 6H), 1.48 (m, 6H), 1.30 (m, 24H), 0.88 (t, 9H). ^{13}C NMR ($CDCl_3$): δ = 153.9, 144.3, 136.5, 135.3, 123.5, 116.6, 112.4, 101.9, 73.7, 69.4, 32.0, 30.5, 29.7, 26.2, 22.8, 14.2. MS: m/z = 640.7 (M^+).

*Synthesis of (−)-N-[3,4,5-Tri((S)-3,7-dimethyloctyloxy)phenyl]dithieno[3,2-b:2′,3′-d]pyrrole (**4b**).* The same procedure was followed as described for the synthesis of **4a**, starting from **3b** (4.00 g, 7.20 mmol). The product was isolated as a colorless oil. Yield: 2.70 g (52%); $[\alpha]_D^{20}$ = −4.21 deg mL g^{-1} dm^{-1} (c = 1.4 in THF). ^{1}H NMR ($CDCl_3$): δ = 7.17 (d, J = 4.6 Hz, 2H), 7.14 (d, J = 4.6 Hz, 2H), 6.75 (s, 2H), 4.02 (m, 6H), 1.81−1.95 (m, 3H), 1.45−1.80 (m, 9H), 1.10−1.40 (m, 18H), 0.96 (m, 9H), 0.87 (m, 18H). ^{13}C NMR ($CDCl_3$): δ = 153.9, 144.2, 136.6, 135.3, 123.4, 116.6, 112.3, 101.8, 71.9, 67.6, 39.4, 37.6, 36.4, 29.9, 28.1, 24.8, 22.7, 19.8. MS: m/z = 725.1 (M^+).

*Synthesis of 2,6-Diiodo-N-[3,4,5-tri(octyloxy)phenyl]dithieno[3,2-b:2′,3′-d]pyrrole (**5a**).* At 0 °C, NIS (990 mg, 0.440 mmol) was added to a solution of **4a** (0.128 g, 0.200 mmol) in $CHCl_3$ (2 mL). After stirring for 15 min, the mixture was allowed to warm to room temperature. The reaction was monitored by TLC (eluens: CH_2Cl_2/hexane (50/50)). After 2 h, another portion of NIS (9.90 mg, 0.0440 mmol) was added. The mixture was stirred for an additional 2 h, and a solution of $NaHSO_3$ in H_2O (10 mL) and CH_2Cl_2 (20 mL) was added. The aqueous layer was separated and extracted with CH_2Cl_2 (20 mL). The combined organic layers were washed with H_2O and dried over $MgSO_4$. After filtration and removal of the organic solvents by rotary evaporation, the crude product was purified by column chromatography (SiO_2, CH_2Cl_2/hexane (50/50)) to obtain a viscous oil. Yield: 0.140 g (78%). ^{1}H NMR ($C_2D_2Cl_4$): δ = 7.26 (s, 2H), 6.60 (s, 2H), 3.95 (m, 6H), 1.80 (m, 6H), 1.47 (m, 6H), 1.27 (m, 18H), 0.87 (m, 9H). ^{13}C NMR ($CDCl_3$): δ = 154.0, 143.3, 137.3, 134.4, 121.5, 120.8, 102.5, 73.8, 71.4, 69.6, 32.0, 30.5, 29.5, 26.3, 22.9, 14.3. MS: m/z = 892.4 (M^+), 765.8 (M^+ − I).

*Synthesis of (−)-2,6-Diiodo-N-[3,4,5-tri((S)-3,7-dimethyloctyloxy)phenyl]dithieno[3,2-b:2′,3′-d]pyrrole (**5b**).* The same procedure as described for **5a** was followed, starting from **4b** (0.300 g, 0.410 mmol). The product was isolated as a colorless oil. Yield: 0.280 g (71%). $[\alpha]_D^{20}$ = −4.03 mL g^{-1} dm^{-1} (c = 1.2 in THF). ^{1}H NMR ($C_2D_2Cl_4$): δ = 7.18 (s, 2H), 6.54 (s, 2H), 3.91 (m, 6H), 1.78−1.92 (m, 3H), 1.44−1.76 (m, 9H), 1.09−1.39 (m, 18H), 0.86 (m, 9H), 0.78 (m, 18H). ^{13}C NMR ($CDCl_3$): δ = 154.3, 143.5, 137.6, 134.7, 121.7, 121.1, 102.7, 72.3, 71.7, 68.2, 39.7, 37.8, 36.7, 30.2, 28.4, 25.1, 23.1, 20.1. MS: m/z = 976.4 (M^+), 849.9 (M^+ − I).

*Synthesis of 2,6-Di(trimethyltin)-N-[3,4,5-tri(octyloxy)phenyl]dithieno[3,2-b:2′,3′-d]pyrrole (**6a**).* At 0 °C, a solution of **4a** (0.640 g, 1.00 mmol) in dry Et_2O (40 mL) was purged with argon, and *t*-BuLi (1.40 mL, 2.10 mmol, 1.5 M in pentane) was added dropwise, resulting in the formation of a white precipitate. The mixture was allowed to reach room temperature, and after stirring for 15 min, a solution of Me_3SnCl (0.438 g, 2.20 mmol) in dry Et_2O (5 mL) was added. The initial white precipitate disappeared, and initially a yellowish, clear solution was obtained, from which another white precipitate formed. After stirring at room temperature for 1 h, the solvents were removed. Hexane was added, and the mixture was filtered, hereby removing inorganic salts. The crude product was precipitated in MeOH at −78 °C and filtered off. It melts near −15 °C, leaving a viscous oil at room temperature. Yield: 0.820 g (85%). ^{1}H NMR ($CDCl_3$): δ = 7.14 (s, 2H), 6.78 (s, 2H), 4.01 (m, 6H), 1.83 (m, 6H), 1,49 (m, 6H), 1,26 (m, 24H), 0.89 (t, 9H), 0.39 (s, 18H). ^{13}C NMR ($CDCl_3$): δ = 153.8, 147.2, 136.7, 135.8, 122.3, 119.2, 102.5, 73.8, 69.6, 32.0, 30.5, 29.5, 26.2, 22.8, 14.2, −8.0. MS: m/z = 966.6 (M^+), 640.7 (M^+ − $Sn_2C_6H_{16}$).

*Synthesis of (−)-2,6-Di(trimethyltin)-N-(3,4,5-tri((S)-3,7-dimethyloctyloxy)phenyl)dithieno[3,2-b:2′,3′-d]pyrrole (**6b**).* The same procedure was followed as described for **6a**, starting from **4b** (0.500 g, 0.690 mmol). The product was isolated as a pale yellow, viscous oil. Yield: 0.630 g (86%). $[\alpha]_D^{20}$ = −8.49 deg mL g^{-1} dm^{-1} (c = 1.4 in THF). ^{1}H NMR ($CDCl_3$): δ = 7.15 (s, 2H), 6.79 (s, 2H), 4.03 (m, 6H), 1.89 (m, 3H), 1.50−1.79 (m, 9H), 1.08−1.40 (m, 18H), 0.95 (m, 9H), 0.87 (m,18H), 0.39 (s, 18H). ^{13}C NMR ($CDCl_3$): δ = 153.8, 147.1, 136.6, 136.4, 135.8, 122.3, 119.2, 102.2, 72.0, 67.8, 39.4, 37.5, 36.5, 29.9, 28.1, 24.9, 22.8, 19.7, −8.0. MS: m/z = 1049.9 (M^+), 725.0 (M^+ − $Sn_2C_6H_{16}$).

Synthesis of the Polymers. *Synthesis of Poly(N-[3,4,5-tri(octyloxy)phenyl]dithieno[3,2-b:2′,3′-d]pyrrole) (**Pa**).* A solution of **6a** (96.4 mg, 0.100 mmol) and **5a** (89.1 mg, 0.100 mmol) in dry toluene was added to a suspension of CuO (7.9 mg, 0.10 mmol) and $Pd(PPh_3)_4$ (5.8 mg, 5.0 μmol) in dry DMF (5 mL). The reaction mixture was purged with argon for 30 min at room temperature, after which it was refluxed for 15 h. Upon heating, the yellow solution turned from fluorescent red to dark purple. After cooling, the polymer was precipitated in MeOH (100 mL) and filtered. It was fractionated by Soxhlet extractions using subsequently acetone, hexane, and THF. The THF fraction, being the high-molecular-

Scheme 1. Monomer Synthesis

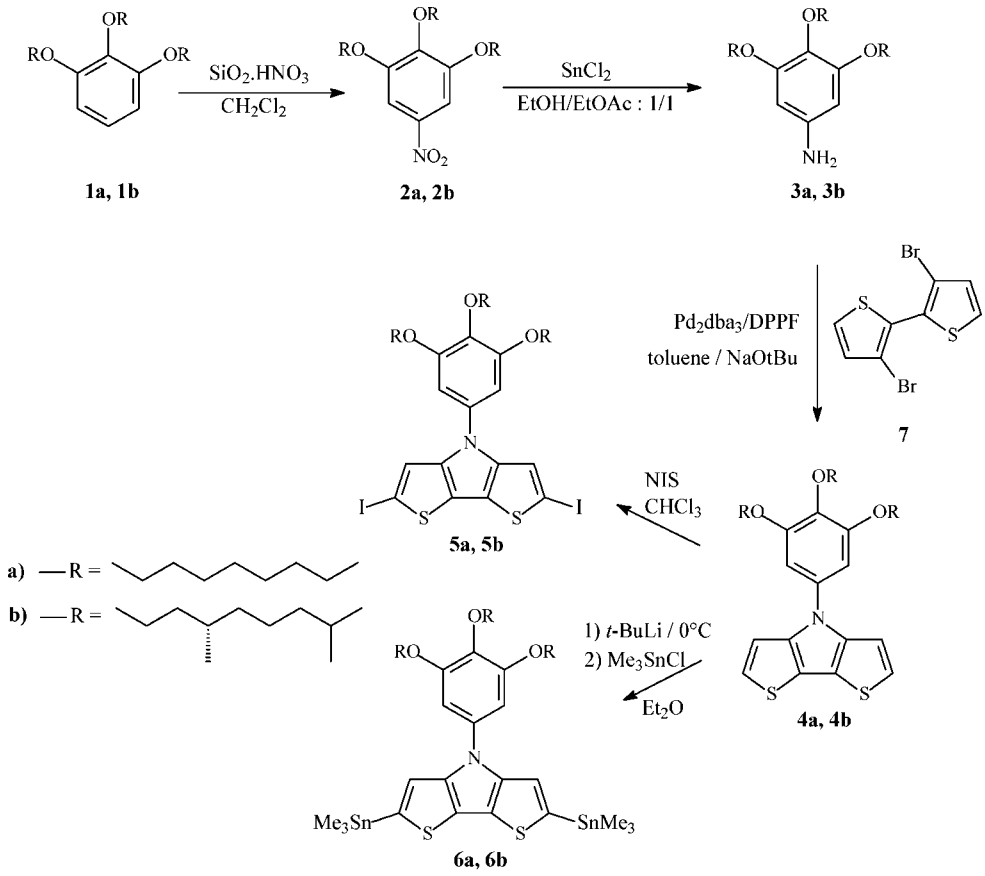

weight fraction, was concentrated in vacuo, and the polymer was precipitated in MeOH. Filtration and drying under vacuum yielded a black solid.

*Synthesis of Poly(N-[3,4,5-tri((S)-3,7-dimethyloctyloxy)phenyl]dithieno[3,2-b:2′,3′-d]pyrrole) (***Pb***).* The same procedure as described for **Pa** was followed, starting from **6b** (105 mg, 0.10 mmol) and **5b** (97.5 mg, 0.10 mmol).

Results and Discussion

Synthesis. The N-substituted dithienopyrrole monomers were prepared from 3,3′-dibromo-2,2′-bithiophene[10] and the appropriate amines using a Buchwald−Hartwig reaction (Scheme 1). The advantage of this approach is that variation of the substituent only requires the last step of the reaction sequence to be repeated.[12] As already stated, a tri(alkyl)-substituted gallic acid moiety was employed instead of (branched) alkyl groups, in order to induce a helical conformation. The use of chiral alkyl chains in the gallic acid moiety should ensure a preferred helical handedness. Furthermore, this group increases the solubility of the polymers in common organic solvents. For these particular amines, DPPF was used instead of BINAP, since this modification afforded higher yields. The desired amines **3a** and **3b** were synthesized according to a slightly modified literature procedure.[11]

The polymers **Pa** and **Pb** were prepared using a Stille coupling (Scheme 2). A Stille coupling was preferred and not, for instance, polymerization using chemical oxidants, since (i) the former method fully excludes $\alpha-\beta$ coupling and (ii) higher degrees of polymerization can be obtained.[5f] The used polymerization conditions (toluene/DMF (1/1) as solvent, $Pd(PPh_3)_4$ as catalyst, and addition of CuO) appeared to allow a high degree of polymerization and good yields. After polymerization, the polymers were precipitated in MeOH and extracted with subsequently acetone, hexane, and THF using a Soxhlet

Scheme 2. Polymer Synthesis

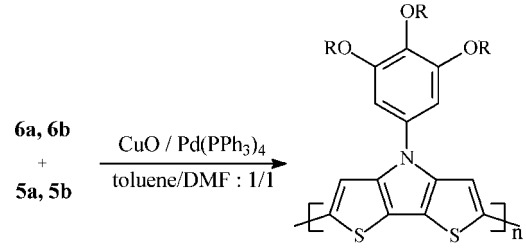

apparatus. Finally, the high-molecular-weight fraction (being the THF fraction) was precipitated in MeOH. In this way, high-molecular-weight **Pa** and **Pb** could be prepared in 44% and 50% yield, respectively.

^{1}H NMR spectroscopy confirms the proposed molecular structure. A representative spectrum of **Pb** is shown in Figure 2. It is clear that no defects or end groups are present, confirming the regular structure and high degree of polymerization.

DSC and GPC Analysis. DSC experiments reveal that both polymers do not degrade or melt below 280 °C. For **Pb**, a glass transition was observed at 143 °C (scanning rate = 20 °C/min.). By GPC, extremely high molecular weights are measured (for **Pa**: $\bar{M}_n = 8.7\ 10^2$ kg mol^{-1}; for **Pb**: $\bar{M}_n = 4.8\ 10^3$ kg mol^{-1}, toward polystyrene standards in THF). Then again, one must take into account that GPC determines the hydrodynamic volume, which is very conformation-dependent. As the molecular weights are determined toward polystyrene standards, which adopt a coil-like conformation while **Pa** and **Pb** adopt a rigid-rod-like conformation in THF (as will be shown later), an overestimation of the molecular weight, determined by GPC, can be expected.[13] Therefore, also MALDI-TOF measurements

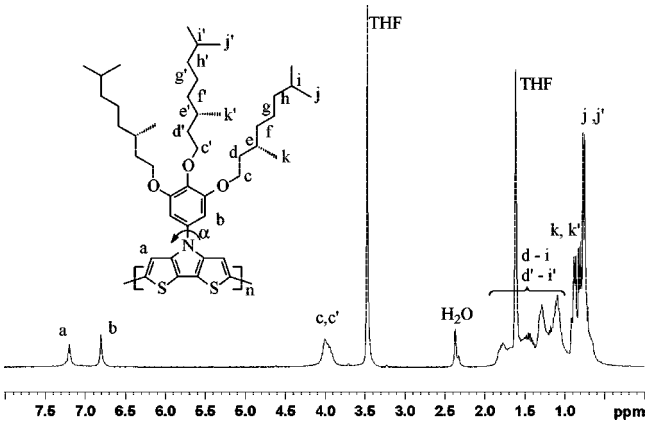

Figure 2. ^{1}H NMR spectrum of **Pb** in THF-d_8.

were carried out. Unfortunately, only the low-molecular-weight fraction could be ionized, rendering an extremely underestimated molecular weight by MALDI-TOF ($\bar{M}_n \sim 5120$ g mol^{-1}). However, the fact that no end groups are detected in the ^{1}H NMR spectrum (Figure 2) indicates that the polymer is of high molecular weight. Indeed, if the polymers are terminated by a trimethyltin-functionalized DTP, trimethyltin groups or doublets in the aromatic region, arising from a destannylated DTP moiety, are expected. Diiodo-DTP-terminated polymer strands would give rise to an additional singlet in the aromatic region. None of these end groups can be distinguished. Finally, high degrees of polymerization are also consistent with the high conjugation length ($\lambda_{max} \sim 560$ nm, see later) in THF, whereas previously prepared low-molecular-weight poly(dithienopyrrole)s (~5 repeating units, as confirmed by MALDI-TOF) show a lower conjugation length ($\lambda_{max} \sim 530$ nm).[5d]

Optical Properties. The combination of several spectroscopic techniques can be very useful for the determination of the supramolecular behavior of conjugated polymers. For instance, combined UV−vis, CD, and emission spectroscopy enabled us to demonstrate that alkyl-substituted PDTPs adopt a strongly conjugated, rigid-rod-like conformation in a good solvent and (chirally) aggregate upon addition of nonsolvents.[5f] In order to be able to use CD spectroscopy, all optical measurements were done using the chiral polymer **Pb**.

A representative UV−vis spectrum of **Pb** in THF, a good solvent for these polymers, is shown in Figure 3a. The comparison of the UV−vis spectrum of an alkyl-substituted PDTP and **Pb** can be very helpful for assigning all absorption bands to their corresponding transitions. Therefore, also the UV−vis spectrum of the previously reported poly(*N*-[1-(octyloxymethyl)propyl]dithieno[3,2-*b*:2′,3′-*d*]pyrrole) (**Palk**)[5f] is incorporated. Both polymers show an absorption band near 550 nm, which can be ascribed to the $\pi-\pi^*$ transition, located on the polymer backbone. Moreover, from the similarly high λ_{max}, it is clear that also **Pb** adopts a highly conjugated conformation in a good solvent. Further comparison of both spectra reveals that the absorption at 350 nm is attributed to a (localized) transition on the polymer main chain as well, while the absorption at 267 nm, which is absent for alkyl-substituted PDTPs, must originate from the gallic acid moiety, located on the side chain.

Emission spectroscopy is an interesting tool to probe the rigidity of the polymer backbone since fwhm$_{em}$ and the Stokes shift decrease with increasing rigidity. In THF, a small fwhm$_{em}$ and Stokes shift are observed for **Pb** (fwhm$_{em}$ = 1147 cm^{-1}, Stokes shift = 1517 cm^{-1}), similarly as for **Palk**, indicating that **Pb** also adopts a rigid structure. Circular dichroism (CD), finally, is a useful tool to study the chiral (supra)molecular structure, since the

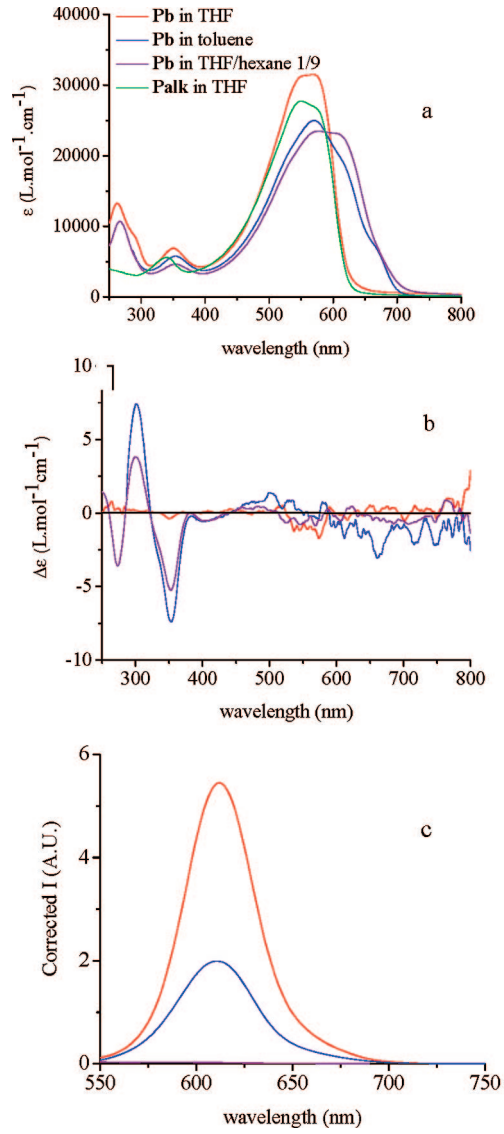

Figure 3. (a) UV−vis, (b) CD, and (c) fluorescence spectra (excitation wavelength 530 nm (THF and toluene) and 590 nm (THF/hexane)) of **Pb** in THF (c = 21.6 mg/L), toluene (c = 16.0 mg/L), and THF/hexane 1/9 (c = 33.6 mg/L)). The fluorescence intensity I is corrected for the polymer concentration and refraction index of the solvent used. (a) UV−vis spectrum of **Palk** in THF (c = 16.0 mg/L).

presence of Cotton effects is a direct proof for chiral (orientation of) chromophores.[14] In THF solution, no CD effects are observed for **Pb**, indicating that there is no chiral order present (Figure 3b). From these experiments, it can be concluded that the gallic acid-functionalized PDTPs adopt a rigid, strongly conjugated conformation in good solvents, such as THF.

The addition of *n*-hexane (a nonsolvent) to the THF solution leads to a small red shift of the $\pi-\pi^*$ transition in the UV−vis spectrum (Figure 3a), indicating a (slight) increase of the conjugation length, probably arising from a planarization of the polymer backbone. The transition at 351 nm, however, is unaffected by the addition of nonsolvent, although it is located in the main chain. This confirms that it is localized on a DTP monomeric unit and, consequently, not influenced by changes in the torsion angle between adjacent units. Also the transition of the side chain at 267 nm is unaffected by the solvent change. Interestingly, toluene (neat) provokes a similar behavior as THF−hexane (1/9) mixture.

The CD spectra of **Pb** in both the THF−hexane (1/9) mixture and toluene show a bisignate Cotton effect with zero crossing at 284 nm, corresponding to the side-chain transition (Figure

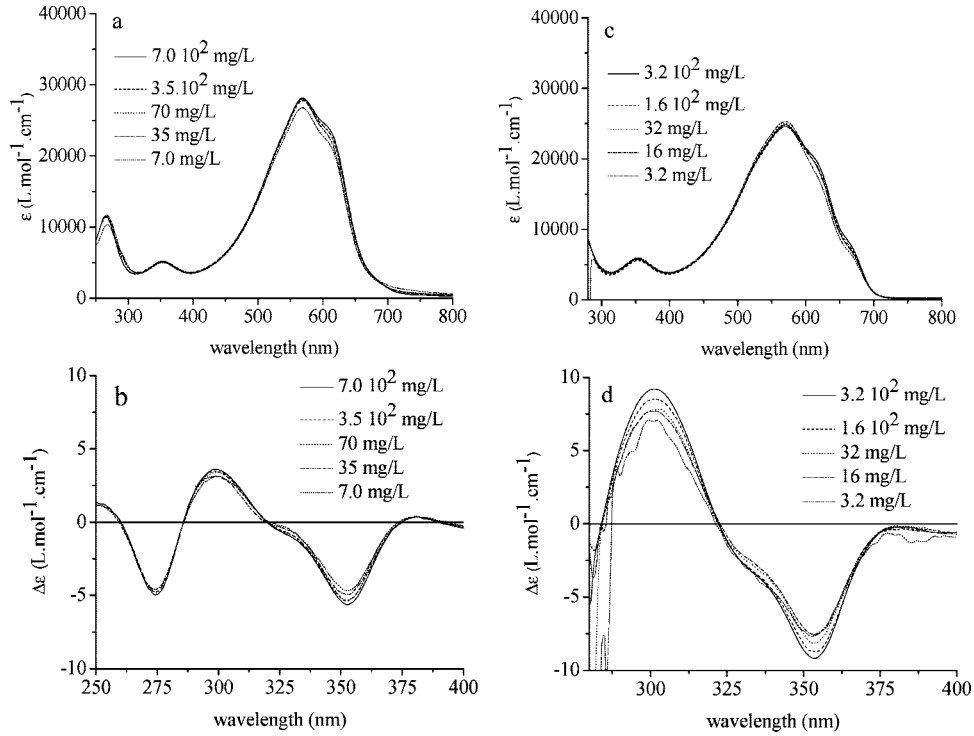

Figure 4. Dilution experiments of **Pb** in THF/hexane (3/7) (a, UV−vis; b, CD) and toluene (c, UV−vis; d, CD).

3b). Since bisignate Cotton effects arise from exciton coupling of chirally ordered chromophores,[14,15] these results directly indicate that the side chains are chirally ordered with respect to each other under these conditions. Also, a monosignate Cotton effect at 353 nm, corresponding to the localized main chain transition, can be distinguished, showing that the monomeric units are part of a chiral setting. Peculiarly, no CD is observed for the $\pi-\pi^*$ transition. It is also worthwhile to note that, although the absolute value for the Cotton effects are rather small, the *g*-value ($\Delta\varepsilon/\varepsilon$) is in the order of 10^{-3}, which is a rather common value.

In the THF/hexane mixture (1/9), the fluorescence is completely quenched (Figure 3c), while in toluene, a very strong fluorescence is observed. The quenching of the fluorescence in THF/hexane is probably due to π-stacking of the emitting chromophores of the polymer backbone, either intramolecularly (due to folding) or intermolecularly (aggregation), induced by addition of hexane, which is a nonsolvent for the aromatic backbone. The emission bands in toluene are again narrow ($fwhm_{em} = 1292\ cm^{-1}$), and the Stokes shifts are small (1151 cm^{-1}), pointing at a rigid backbone.

It is clear that the supramolecular behavior of **Pb** in THF, in which the polymer is present as rigid, disordered rods, significantly differs from the situation in THF−hexane (1/9) and toluene. The presence of the Cotton effects in the latter solvents unambiguously points at the presence of chirality. Two possibilities now arise: either it is supramolecular (helical stacks of different polymer chains) or macromolecular (a one-handed helical conformation) in nature. In the former case, the UV−vis and CD spectra must be concentration dependent, while in the latter case, a concentration independence will be observed. To discriminate between both, dilution experiments were carried out in THF/hexane and toluene (Figure 4). In this respect, the ratio THF/hexane was first varied, which revealed that a THF/hexane (3/7) ($c = 33.6$ mg/L) displays intermediate UV−vis and CD spectra (Supporting Information, Figure S1). Consequently, the dilution measurements for THF/hexane were performed in this solvent mixture. Both in toluene and THF/hexane 3/7, only minor changes in the UV−vis and CD spectra are observed over a broad concentration range (100-fold dilution), ruling out the possibility of supramolecular chirality in both solvents (Figure 4).

All experimental data support the hypothesis, as mentioned in the introduction, that the incorporation of the gallic acid-derived moiety as side chains in PDTP gives rise to a helical conformation in the appropriate solvent (THF/hexane and toluene). As the polymer backbone adopts a helical conformation, the phenyl side chains become helically wrapped around the polymer backbone, which explains the observed bisignate Cotton effect at 267 nm. The chiral (helical) setting of the monomeric units, on the other hand, gives rise to the monosignate Cotton effect at 353 nm. In general, it seems that the incorporated gallic acid-derived moiety favors a helical conformation over aggregation.

Since the angle between two adjacent DTP units is quite small, it can be expected that a rather large number of repeating units are present in one turn and that, consequently, the diameter can be expected to be fairly large as well. First, this can explain the red shift in the $\pi-\pi^*$ transition, observed for the transition to the helical conformation: the torsion angle between adjacent monomeric units is in this conformation very small. Second, the absence of a Cotton effect in the $\pi-\pi^*$ transition of the polymer backbone can be correlated to the fact that the helical turn, being very wide, approximates a circle, being achiral and thus CD silent. Third, the regularity of this structure can explain the presence of some vibronic side bands in the UV−vis spectra, while the small emission bands and Stokes shifts can be attributed to its rigidity. Finally, the difference in emission intensity between toluene and THF/hexane could be correlated to the ability of the solvent to interact with aromatic moieties. In this respect, toluene is a far better solvent than hexane, and as a consequence, the resulting helical conformation in THF/hexane could be more compact then in toluene, which results in quenching of the emission. Therefore, these results might indicate that the helical conformation can be "fine-tuned" by the choice of the solvent (Figure 5).

In a broader view, substituted PDTPs constitute an archetype of how the substituent can govern the (supra)molecular behavior

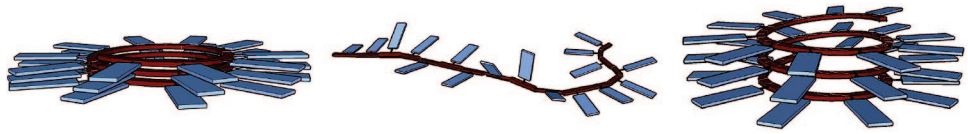

Figure 5. Schematic representation of **Pb** in THF/hexane (left), THF (middle), and toluene (right).

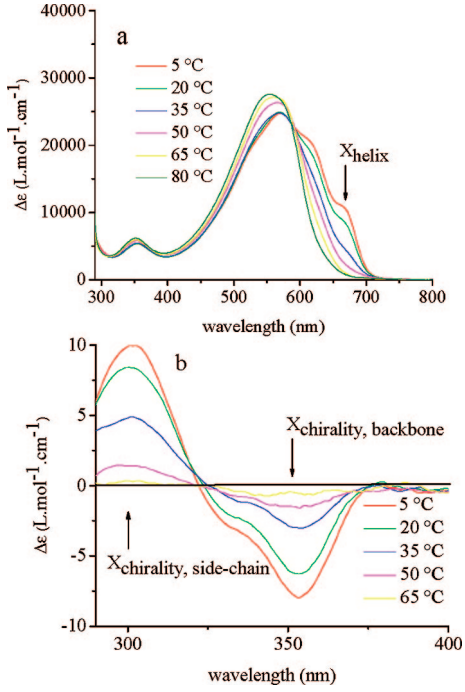

Figure 6. Temperature-dependent (a) UV−vis and (b) CD spectra of **Pb**, starting at 5 °C. The solution was first kept at 5 °C for 40 h.

of (conjugated) polymers. If linear or slightly branched alkyl side chains are used, only low-molecular-weight, soluble PDTPs are obtained. The poor solubility of these materials can be attributed to strong π-stacking. If, however, more branched side chains are incorporated, the π-stacking is diminished, which results in higher yields and molecular weights. These PDTPs adopt a strongly conjugated, rigid-rod-like conformation in solution and aggregate upon addition of nonsolvents. Chirality, if present, is supramolecular in nature (chiral aggregation). However, as mentioned above, substitution with a gallic acid moiety induces macromolecular chirality (one-handed helical conformation) under appropriate conditions. As a consequence, these findings demonstrate that the conformation and supramolecular structure of the polymer, which play a crucial role for the eventual properties and applications of the polymer—supramolecular aggregation is, for instance, favorable for FETs, etc., while chiral sensing is typically found for helical polymers—can be governed by a proper choice of the substituent, without any adaptation of the conjugated backbone itself.

A Comparative UV−vis and CD Study of the (Un)folding Behavior. Apart from the solvent (solvatochroism), also temperature plays an important role in a helix−coil transition (thermochroism).[3a,16] The temperature dependence of the UV−vis and CD spectra of **Pb** in toluene, showing this transition, are displayed in Figure 6. From these spectra, it is clear that the polymer adopts a random-coil conformation at high temperature ($T \geq 85$ °C), while below 10 °C, it is (solely) present as chiral helices. Cooling below 10 °C or heating above 85 °C does not alter the spectra, indicating that the transition is completed within the range 10 °C $\leq T \leq$ 85 °C and that the polymer is fully present as random coils at high temperature and as chiral helices at low temperature.

On the other hand, these findings do not reveal anything about the mechanism of the helix−coil transition. One might, for instance, speculate on a multistep folding mechanism, in which the polymer backbone is first folded into a one-handed helix, acting as a template for the chiral ordering of the side chains. Alternatively, some side chains might first chirally stack, forming a nucleus from which the polymer backbone folds into a chiral helix. The third possibility could be the formation of right- and left-handed helices—in racemic ratios—which resolve in a second step. Finally, the helix−coil transition observed could be a single-step process.

Interestingly, the folding and unfolding mechanism in these polymers can be revealed by a combination of UV−vis and CD spectroscopy. Since the polymer backbone absorbs at 667 nm in its helical conformation while it does not in its coil-like state, probing the absorbance at 667 nm gives direct information on the ratio of helices presented. On the other hand, it does not disclose anything about the chirality of the polymer backbone (enantiomeric excess of the helices present) nor about the side chain. Second, the ellipticity at 353 nm is solely related to the chirality of the DTP moieties, present in the polymer backbone, and it therefore probes the chirality of the polymer backbone (enantiomeric excess of the helices present). Finally, the ellipticity at 300 nm (the positive, low-energy lobe of the 267 nm absorption) originates from the chiral ordering of the side chain and probes therefore the chiral stacking of the side chain, independently from the conformation and/or chirality of the polymer backbone. Therefore, the following parameters are defined:

$$X_{\text{helix}} = \frac{\varepsilon_{667,T} - \varepsilon_{667,C}}{\varepsilon_{667,H} - \varepsilon_{667,C}} \quad (1)$$

$$X_{\text{chirality,backbone}} = \frac{\Delta\varepsilon_{353,T}}{\Delta\varepsilon_{353,H}} \quad (2)$$

$$X_{\text{chirality,side chain}} = \frac{\Delta\varepsilon_{300,T}}{\Delta\varepsilon_{300,H}} \quad (3)$$

in which $\varepsilon_{667,T}$, $\varepsilon_{667,C}$, and $\varepsilon_{667,H}$ denote for the extinction coefficient at 667 nm at temperature T, the extinction coefficient of the random-coil polymer (measured at $T = 85$ °C), and the extinction coefficient of the helical polymer (measured at $T =$ 10 °C), respectively. Likewise, $\Delta\varepsilon_{353,H}$ denotes for the ellipticity at 353 nm in the helix conformation ($T = 5$ °C). $\Delta\varepsilon_{300,H}$, finally, denotes for the ellipticity at 300 nm in the helix conformation. As a consequence, X_{helix}, $X_{\text{chirality,backbone}}$, and $X_{\text{chirality,side chain}}$ represent the fraction of helices, the fraction of *chiral* helices and the fraction of chirally oriented side chains, present at temperature T, respectively.

Consequently, a plot of X_{helix}, $X_{\text{chirality,backbone}}$, and $X_{\text{chirality,side chain}}$ vs temperature can elucidate the folding and unfolding mechanism of this polymer. A multistep process would be reflected by a discrepancy of the parameters, while three simultaneous transitions point at a single-step transition. For instance, if $X_{\text{chirality,side chain}}$ starts to increase at lower temperature in the cooling cyclus (coil → helix transition), this would reflect that the side chains first preorganize, from which the polymer backbone folds.

Therefore, UV−vis and CD spectra were recorded at several temperatures ranging from 10 to 85 °C. The data points were measured twice, starting from a freshly prepared solution, to

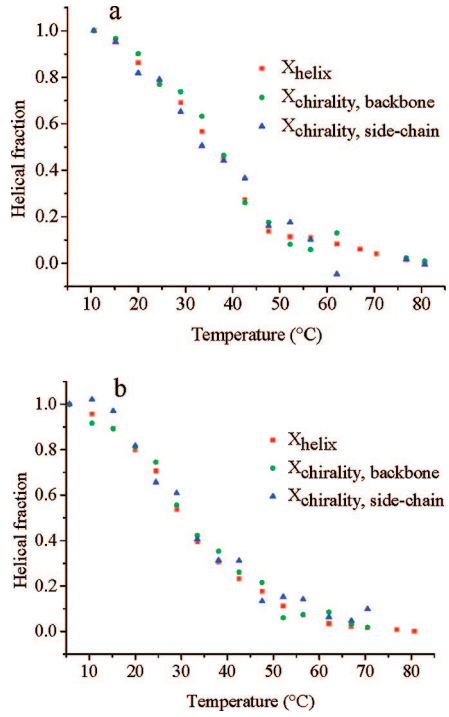

Figure 7. Temperature dependence of X_{helix}, $X_{chirality,backbone}$, and $X_{chirality,side\ chain}$: (a) cooling and (b) heating.

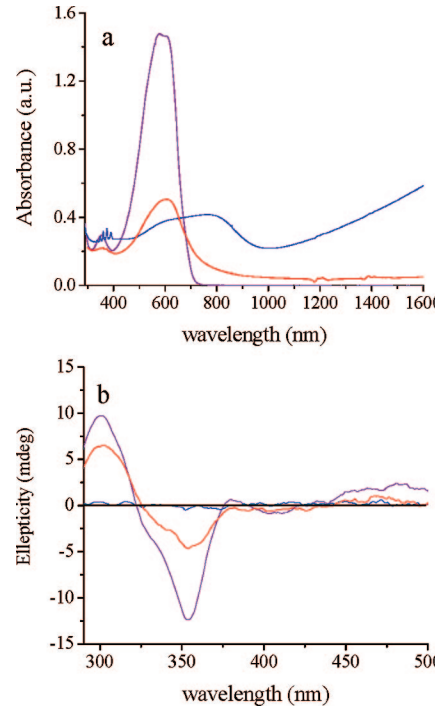

Figure 8. (a) UV−vis and (b) CD spectra of **Pb** (37 mg/L) in THF/hexane 1/9 in its neutral (purple line), oxidized (blue line), and rereduced (red line) state.

ensure the reproducibility. To exclude any kinetic effects, all spectra were recorded until no change was observed. For the lowest temperatures in the cooling cyclus, this could take up to 40 h. The requirement of this long period of time can be explained by the rigidity of the polymer backbone (vide supra), which slows down the movement of the polymer, especially at low temperatures.

Figure 7 shows a plot of X_{helix}, $X_{chirality,backbone}$, and $X_{chirality,side\ chain}$ vs temperature for the coil → helix transition (cooling) and helix → coil transition (heating). First, the spectra show only dependency on the temperature and not on their history (cooling or heating). This again confirms that no kinetic issues are involved and that each data point corresponds to the thermodynamically most stable situation. Second, it is clear that the coil−helix transition is a single-step process, as all three parameters show, within experimental errors, the same temperature dependence. This is fully in line with the previously stated hypothesis that rigid polymers can exhibit first-order (two-state) transitions at thermal equilibrium.[3b,17] The data fit well in a Van't Hoff plot, from which $\Delta H^{\#} = -92$ kJ/mol and $\Delta S^{\#} = -0.30$ kJ/(mol K) can be estimated for the coil → helix transition (Supporting Information, Figure S6). It is worthwhile to mention that these findings do not necessarily conflict with the Zimm−Bragg coil-helix model ($\Delta G = \sigma s^{n-n0}$),[18] in which first a nucleus is formed in a first step (this contribution is reflected by "σ"), from which the helix propagates (this is reflected by "s^{n-n0}"). In the helical PDTPs, the nucleus formation can expected to be negligible compared to the helix propagation since (i) the entropy change during the nucleus formation is small due to the rigidity of the polymer backbone (i.e., σ is small) and (ii) every nucleus gives rise to a very large number of helix propagations, since n (= degree of polymerization) is very large. Therefore, only the helix propagation is observed.

Apart from optical techniques, also ^{1}H NMR spectroscopy can provide further evidence for the conformational changes. For instance, protons under or above an aromatic ring experience an upfield shift, and therefore, the helix formation can lower the chemical shift of some protons.[3a] A ^{1}H NMR spectrum of **Pb** in toluene at 80 °C reveals two distinguishable signals for $H_{c'}$ and H_c (for the designation of the protons, see Figure 2) at 4.29 and 4.10 ppm, respectively (Supporting Information, Figure S2), which resembles the spectrum in THF. Decreasing the temperature of the toluene solution and thus inducing helix formation diminishes the 4.10 ppm resonance; instead, a new signal at 3.93 ppm appears. Also, the aromatic H_b is slightly shifted to lower δ. From Figure 7, it is clear that at 80 °C **Pb** is fully present as a random coil, whereas at 25 °C the strands adopt mainly a helical conformation with some unorganized parts still present. The decrease of δ by helix formation can be explained by an increase of the angle between the gallic acid and DTP moieties (α, Figure 2), which alters the electronic environment of these protons, which is to a large extent determined by the magnetic anisotropy arising from the DTP nucleus. $H_{c'}$, being located on the rotation axis of α, is unaffected by a change of this angle.

Apparently, the helical pitch in toluene is too large for the shift of the aromatic protons to be influenced by the under- and above-lying aromatic rings. In contrast, the helix is more "compact" in THF/hexane mixtures. Indeed, an ^{1}H NMR spectrum in a THF/hexane 3/7 mixture shows severe line broadening and an unresolved, very broad absorption band in the aromatic region (Supporting Information, Figure S4), which is in full agreement with a large helical pitch in toluene but a very dense structure in THF/hexane.

Oxidation of the PDTP Backbone. Finally, **Pb** was oxidized in a THF/hexane mixture (1/9), in which the polymer is thus present as a one-handed helix (Figure 8). The oxidation was accomplished using $NOBF_4$ as an oxidant, which was preferred compared to I_2, to avoid spectral interference from the I_3^- or I_5^- counterion. After oxidation, the polymer was back reduced with hydrazine. The ease with which the polymer can be oxidized can be correlated with its low $E_{1/2}$ (0.76 V), as measured by cyclic voltammetry on film samples of **Pb**, scan rate = 100 mV/s, vs SCE (3 M KCl) (Supporting Information, Figure S5).

Unfortunately, the addition of $NOBF_4$ leads to partial precipitation of oxidized polymer. Upon addition of hydrazine, a polymer film at the water−THF/hexane interface is formed.

This explains the decrease in absorbance of the back-reduced, neutral state compared with the original, neutral state. In toluene, the precipitation is even more severe, and as a consequence, recording these spectra is not feasible. On the other hand, it is clear that no degradation of the polymer takes place, since the original shape of the spectra, both UV−vis and CD, is restored.

Interestingly, the oxidized polymer shows no circular dichroism. For the localized main chain transition near 353 nm, one might attribute this to the fact that its transition is affected by oxidation or that chirality is lost. The side-chain transition absorbance, however, is less affected by oxidation of the polymer backbone, and as a consequence, the disappearance of (bisignate) Cotton effects must point at a loss of chirality. This is consistent with neutral **Pb** having a helical conformation: oxidation induces further planarization of the main chain (to delocalize the positive charges) and alters the (helical) conformation. The loss of the chiral, helical conformation is accompanied by a loss of chiral ordering of the substituents. Consequently, this explains the disappearance of the Cotton effects of both the main chain and side chain.

The problem of conformational changes due to oxidation could be tackled, which is done in an ongoing study, by using polymer films, as this restricts movement of the polymer chains.[5d,6c]

Conclusion

In conclusion, we have prepared poly(dithienopyrrole)s (PDTPs) which are functionalized with a (chiral) gallic acid derivative and studied their conformational behavior in solution. The polymers were prepared by a Stille coupling. In good solvents (e.g. THF), the polymers adopt a strongly conjugated, rigid, probably rodlike conformation. In poor solvents (a THF/hexane (1/9) mixture or toluene) the polymer adopts a one-handed (in the case of chiral polymers) helical conformation, which is in contrast to previously reported alkyl-substituted PDTPs, which aggregate in nonsolvents. The helix formed in THF/hexane is probably more densely packed than in toluene, as demonstrated by emission spectroscopy. The folding and unfolding of the helix was monitored by UV−vis and CD spectroscopy and appeared to proceed via a single-step process. Finally, the reversal oxidation of the polymer in its helical conformation was studied, which revealed that the helix unfolds upon oxidation but folds back when reduced. Further research will focus on the chiroptical properties and conformational behavior in film.

Acknowledgment. We are grateful to the Katholieke Universiteit Leuven (GOA), the Fund for Scientific Research (FWO-Vlaanderen), and Toyota Motor Co. for financial support and to dr. Jurgen Huybrechts for the MALDI-TOF experiments. K.V.d.B. is a doctoral fellow of IWT, and G.K. is a postdoctoral fellow of the Fund for Scientific Research (FWO-Vlaanderen).

Supporting Information Available: UV−vis and CD spectra of **Pb** in different THF/hexane mixtures, ^{1}H NMR spectra of **Pb** in different solvents, a CV scan of **Pb**, a Van't Hoff plot of **Pb** in toluene, and ^{1}H NMR spectra of all polymers and compounds and ^{13}C NMR of all new compounds. This material is available free of charge via the Internet at http://pubs.acs.org.

References and Notes

(1) (a) Gellman, S. H. *Acc. Chem. Res.* **1998**, *31*, 173–180. (b) Rowan, A. E.; Nolte, R. J. M. *Angew. Chem., Int. Ed.* **1998**, *37*, 63–68. (c) Green, M. M.; Park, J. W.; Sato, T.; Teramoto, A.; Lifson, S.; Selinger, R. L. B.; Selinger, J. V. *Angew. Chem., Int. Ed.* **1999**, *38*, 3139–3154. (d) Cornelissen, J. J. L. M.; Rowan, A. E.; Nolte, R. J. M.; Sommerdijk, N. A. J. M. *Chem. Rev.* **2001**, *101*, 4039–4070. (e) Fujiki, M. *Macromol. Rapid Commun.* **2001**, *22*, 539–563. (f) Hill, D. J.; Mio, M. J.; Prince, R. B.; Hughes, T. S.; Moore, J. S. *Chem. Rev.* **2001**, *101*, 3893–4011. (g) Nakano, T.; Okamoto, Y. *Chem. Rev.* **2001**, *101*, 4013–4038. (h) Schmuck, C. *Angew. Chem., Int. Ed.* **2003**, *42*, 2448–2452. (i) Yashima, E. *Chem.—Eur. J.* **2004**, *40*, 42–51. (j) Huc, I. *Eur. J. Org. Chem.* **2004**, *1*, 7–29. (k) Kim, H.-J.; Lim, Y.-B.; Lee, M. *J. Polym. Sci., Part A: Polym. Chem.* **2008**, *46*, 1925. (l) Yashima, E.; Maeda, K. *Macromolecules* **2008**, *41*, 3–12.

(2) (a) Maeda, K.; Yashima, K. M. E. *Macromol. Symp.* **2003**, *201*, 135–142. (b) Aoki, T.; Kaneko, T.; Teraguchi, M. *Polymer* **2006**, *47*, 4867–4892. (c) Masuda, T. *J. Polym. Sci., Part A: Polym. Chem.* **2007**, *45*, 165–180. (d) Yashima, E.; Matsushima, T.; Okamoto, Y. *J. Am. Chem. Soc.* **1995**, *117*, 11596–11597. (e) Suzuki, Y.; Shiotsuki, M.; Sanda, F.; Masuda, T. *Macromolecules* **2007**, *40*, 1864–1867. (f) Akagi, K.; Piao, G.; Kaneko, S.; Sakamaki, K.; Shirakawa, H.; Kyotani, M. *Science* **1998**, *282*, 1683. (g) Cheuk, K. K. L.; Lam, W. J. Y.; Chen, J.; Lai, M. L.; Tang, B. Z. *Macromolecules* **2003**, *36*, 5947–5959. (h) Lai, L. M.; Lam, W. J. Y.; Cheuk, K. K. L.; Sung, H. H. Y.; Williams, I. D.; Tang, B. Z. *J. Polym. Sci., Part A: Polym. Chem.* **2005**, *43*, 3701–3706. (i) Schenning, A. P. H. J.; Fransen, M.; Meijer, E. W. *Macromol. Rapid Commun.* **2002**, *23*, 265–270. (j) Aoki, T.; Kaneko, T.; Maruyama, N.; Sumi, A.; Takahashi, M.; Sato, T.; Teraguchi, M. *J. Am. Chem. Soc.* **2003**, *125*, 6346–6347. (k) Percec, V.; Aqad, E.; Peterca, M.; Rudick, J. G.; Lemon, L.; Ronda, J. C.; De, B. B.; Heiney, P. A.; Meijer, E. W. *J. Am. Chem. Soc.* **2006**, *128*, 16365–16372.

(3) (a) Nelson, J. C.; Saven, J. G.; Moore, J. S.; Wolynes, P. G. *Science* **1997**, *277*, 1793–1796. (b) Prince, R. B.; Saven, J. G.; Wolynes, P. G.; Moore, J. S. *J. Am. Chem. Soc.* **1999**, *121*, 3114–3121. (c) Prest, P.-J.; Prince, R. B.; Moore, J. S. *J. Am. Chem. Soc.* **1999**, *121*, 5933–5939.

(4) Goto, H.; Okamoto, Y.; Yashima, E. *Chem.—Eur. J.* **2002**, *8*, 4027.

(5) (a) Berlin, A.; Pagani, G.; Zotti, G.; Schiavon, G. *Macromol. Chem.* **1992**, *193*, 399–409. (b) Zotti, G.; Berlin, A.; Schiavon, G.; Zecchin, S. *Synth. Met.* **1999**, *101*, 622–623. (c) Kenning, D. D.; Ogawa, K.; Rothstein, S. D.; Rasmussen, S. C. *Polym. Mater. Sci. Eng.* **2002**, *86*, 59. (d) Koeckelberghs, G.; De Cremer, L.; Vanormelingen, W.; Verbiest, T.; Persoons, A.; Samyn, C. *Macromolecules* **2005**, *38*, 4545–4547. (e) Ogawa, K.; Rasmussen, S. C. *Macromolecules* **2006**, *39*, 1771–1778. (f) Koeckelberghs, G.; De Cremer, L.; Persoons, A.; Verbiest, T. *Macromolecules* **2007**, *40*, 4173–4181. (g) Berlin, A.; Zotti, G.; Schiavon, G.; Zecchin, S. *J. Am. Chem. Soc.* **1998**, *120*, 13453–13460.

(6) (a) Lemaire, M.; Delabouglise, D.; Garreau, R.; Guy, A.; Roncali, J. *J. Chem. Soc., Chem. Commun.* **1988**, 658. (b) Koeckelberghs, G.; Vangheluwe, M.; Samyn, C.; Persoons, A.; Verbiest, T. *Macromolecules* **2005**, *38*, 5554–5559. (c) Grenier, C. R. G.; George, S. J.; Joncheray, T. J.; Meijer, E. W.; Reynolds, J. R. *J. Am. Chem. Soc.* **2007**, *129*, 10694–10699. (d) Caras-Quintero, D.; Bauerle, P. *Chem. Commun.* **2004**, 926–927.

(7) (a) Havinga, E. E.; Bouman, M. M.; Meijer, E. W.; Pomp, A.; Simenon, M. M. J. *Synth. Met.* **1994**, *66*, 93–97. (b) Majidi, M. R.; Kane-Maguire, L. A. P.; Wallace, G. G. *Polymer* **1994**, *35*, 3113. (c) Reece, D. A.; Kane-Maguire, L. A. P.; Wallace, G. G. *Synth. Met.* **2001**, *119*, 101–102. (d) Su, S.-J.; Takeishi, M.; Kuramoto, N. *Macromolecules* **2002**, *35*, 5752–5757. (e) Yuan, G.-L.; Kuramoto, N. *Chem. Lett.* **2002**, *31*, 544. (f) Goto, H.; Akagi, K. *Macromol. Rapid Commun.* **2004**, *25*, 1482–1486.

(8) Personal communication with dr. J. A. J. M. Vekemans.

(9) Van Gorp, J. J.; Vekemans, J. A. J. M.; Meijer, E. W. *Chem. Commun.* **2004**, 60–61.

(10) Khor, E.; Siu, C. N.; Hwee, C. L.; Chai, S. *Heterocycles* **1991**, *32*, 1805.

(11) (a) Percec, V.; Aqad, E.; Peterca, M.; Rudick, J. G.; Lemon, L.; Ronda, J. C.; De, B. B.; Heiney, P. A.; Meijer, E. W. *J. Am. Chem. Soc.* **2006**, *128*, 16365–16372. (b) Zinsou, A.; Veber, M.; Strezelecka, H.; Jallabert, C.; Fourré, P. *New J. Chem.* **1993**, *17*, 309–313.

(12) (a) Nozaki, K.; Takahasahi, K.; Nakano, K.; Hiyama, T.; Tang, H.-Z.; Fujiki, M.; Yamagushi, S.; Tamao, K. *Angew. Chem., Int. Ed.* **2003**, *42*, 2051–2053. (b) Koeckelberghs, G.; De Cremer, L.; Vanormelingen, W.; Dehaen, W.; Verbiest, T.; Persoons, A.; Samyn, C. *Tetrahedron* **2005**, *61*, 687–691.

(13) Tour, J. M. *Chem. Rev.* **1996**, *96*, 537–553.

(14) Harada, N.; Nakanishi, K. In *Circular Dichroic Spectroscopy*, 1st ed.; University Science Books: Mill Valley, 1983.

(15) Langeveld-Voss, B. M. W.; Beljonne, D.; Shuai, Z.; Janssen, R. A. J.; Meskers, S. C. J.; Meijer, E. W.; Brédas, J.-L. *Adv. Mater.* **1998**, *10*, 1343.

(16) (a) Ciardelli, F.; Lanzillo, S.; Pieroni, O. *Macromolecules* **1974**, *7*, 174–179. (b) Moore, J. S.; Gorman, C. B.; Grubbs, R. H. *J. Am. Chem. Soc.* **1991**, *113*, 1704–1712. (c) Aoki, T.; Kokai, M.; Shinohara, K.-I.; Oikawa, E. *Chem. Lett.* **1993**, 2009–2012. (d) Sanda, F.; Kawasaki, R.; Shiotsuki, M.; Masuda, T. *J. Polym. Sci., Part A: Polym. Chem.* **2007**, *45*, 4450–4458.

(17) Noguchi, H.; Yoshikawa, K. *Chem. Phys. Lett.* **1997**, *278*, 184–188.

(18) Zimm, B. H.; Bragg, J. K. *J. Chem. Phys.* **1959**, *31*, 526–535.

MA8012114